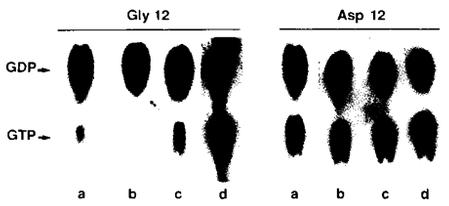

Fig. 5. Stimulation of Gly12 p21 GTPase by mammalian cell extracts. Packed cell pellets were washed with phosphate-buffered saline and lysed with buffer A + 0.5% NP40 (1 vol cell pellet : 0.5 vol lysis buffer). Extracts were mixed with Gly12 or Asp12 p21·GTP and GTPase activities measured as in Fig. 4. Panel a, human peripheral blood lymphocytes; panel b, mouse NIH 3T3 cells; panel c, 1:10 dilution of NIH 3T3 extract in buffer A + 0.5% NP40; and panel d, buffer control.

be considered to be directly upstream from p21 in a signal transduction pathway depending on p21 activation. It is interesting to note that bacterial elongation factor EF-Tu, which may be structurally related to p21 within the GTPase domain (*13*), has virtually no detectable GTPase activity in vitro. As with p21, EF-Tu GTPase activity is greatly stimulated in vivo; in this case by association with ribosome components (*14*).

A striking property of GAP is its failure to stimulate GTPase activity of Asp12 or Val12 p21 proteins. As a result, they are able to remain GTP-bound in vivo. Estimation of GTPase activities of these mutants suggests that they are several hundredfold lower than the GTPase activity of Gly12 p21 in vivo. These differences reflect the different biological potencies of these mutant and normal p21 proteins. We therefore conclude that the major role of Asp12 and Val12 mutations is to prevent interaction with GAP, and that the effects of these mutations on intrinsic GTPase activities measured in vitro are not biologically significant.

REFERENCES AND NOTES

1. E. M. Scolnick *et al.*, *Ann. N.Y. Acad. Sci.* **354**, 398 (1980); V. Manne, S. Yamazaki, H.-F. Kung, *Proc. Natl. Acad. Sci. U.S.A.* **81**, 6953 (1984); M. Gross *et al.*, *Mol. Cell. Biol.* **5**, 1015 (1985).
2. J. B. Gibbs, I. S. Sigal, M. Poe, E. M. Scolnick, *Proc. Natl. Acad. Sci. U.S.A.* **81**, 5704 (1984); J. P. McGrath, D. J. Capon, D. V. Goeddel, A. D. Levinson, *Nature (London)* **310**, 644 (1984); R. W. Sweet *et al.*, *ibid.* **311**, 273 (1984); V. Manne, E. Bekesi, H.-F. Kung, *Proc. Natl. Acad. Sci. U.S.A.* **82**, 376 (1985).
3. A. G. Gilman, *Cell* **36**, 577 (1984).
4. M. Trahey *et al.*, *Mol. Cell. Biol.* **7**, 541 (1987).
5. J. C. Lacal, S. K. Srivastava, P. S. Anderson, S. A. Aaronson, *Cell* **44**, 609 (1986); W. W. Colby, J. S. Hayflick, S. G. Clark, A. D. Levinson, *Mol. Cell. Biol.* **6**, 730 (1986); C. J. Der, T. Finkel, G. M. Cooper, *Cell* **44**, 167 (1986).
6. C. Birchmeier, D. Brock, M. Wigler, *Cell* **43**, 615 (1985).
7. In early experiments, unbound Gpp(NH)p was removed by dialysis before injection of p21·Gpp(NH)p. However, this step was found to be unnecessary, as injection of free Gpp(NH)p (up to 16 m*M*) did not interfere with p21·Gpp(NH)p-induced maturation. Injection of 16 m*M* Gpp(NH)p, GTP, or GDP into oocytes did not induce maturation.
8. J. Maller, M. Wu, J. C. Gerhart, *Dev. Biol.* **58**, 295 (1977).
9. M. E. Furth, L. J. Davis, B. Fleurdelys, E. M. Scolnick, *J. Virol.* **43**, 294 (1982).
10. The cellular GTP pool size in stage VI oocytes has been determined previously by others [M. J. LaMarca, L. D. Smith, M. C. Strobel, *Dev. Biol.* **34**, 106 (1973)] to be on average 257 pmol per oocyte. We attempted to determine the GDP pool size by incubating oocytes in [^{3}H]pool guanosine for 18 hours and resolving labeled nucleotides on PEI Cellulose in 1*M* LiCl. No [^{3}H]GDP could be detected in cellular extracts whereas GTP was labeled efficiently. From these data an upper limit for the GDP pool size can be set at 1/30 of the GTP pool. The GDP and GTP pools rapidly equilibrate as was shown by monitoring the fate of injected [^{3}H]GDP and [^{3}H]GTP. [^{3}H]GDP equilibrated with the GTP pool within 5 minutes. [^{3}H]GTP equilibration with the GDP pool was slower, occurring between 5 and 30 minutes after injection.
11. The ratio of p21·GTP/p21·GDP is a function of GTPase activity (k_{cat}) and GDP dissociation (k_{off}):

$$\text{GTP} + \text{p21} \leftrightarrow \text{p21·GTP} \xrightarrow{k_{cat}}$$

$$\text{p21·GDP} \xrightarrow{k_{off}} \text{p21} + \text{GDP}$$

assuming that when GTP>>GDP, direct binding of GDP to p21 is negligible. At steady state, p21·GTP × k_{cat} = p21·GDP × k_{off}, so, p21·GTP/p21·GDP = k_{off}/k_{cat}. The k_{off} for Gly12, Asp12 and Val12 p21 proteins was measured as follows: 50 μM p21 protein was incubated with 500 μM [8-^{3}H]-GDP (9.3 Ci/mmol, NEN) at 20° for 4 hours. Unbound GDP was removed by dialysis, and p21 GDP was injected into oocytes, as in Fig. 1. We estimated that after dialysis, free [8-^{3}H]GDP amounted to less than 3 pmol per oocyte; this was considered insignificant compared to endogenous guanine nucleotide pools [200 pmol per oocyte (*10*)]. Radiolabeled GDP bound to p21 was recovered as in Fig. 2b. Dissociation $t_{1/2}$'s of about 200 minutes were obtained in each case (k_{off} = ln 2/200). The ratio of p21·GTP/p21·GDP in the experiment shown in Fig. 2a was greater than 5.0. From this, we estimated the hydrolytic half-time to be 1000 minutes.
12. M. Poe, E. M. Scolnick, R. B. Stein, *J. Biol. Chem.* **260**, 3906 (1985).
13. F. Jurnak, *Science* **230**, 32 (1985); F. McCormick *et al.*, *ibid.*, p. 78.
14. J. Gordon, *J. Biol. Chem.* **244**, 5680 (1969).
15. G. Wong *et al.*, *Cancer Res.* **46**, 6029 (1986).
16. M. Wu and J. C. Gerhart, *Dev. Biol.* **79**, 465 (1980).
17. R. W. Merriam, *Exp. Cell Res.* **68**, 75 (1971).
18. The p21, purified by conventional chromatography as described in (*4*) and stoichiometrically bound to GDP was rendered nucleotide-free by dialysis into 10 m*M* EDTA.

19. We thank R. J. Milley for the gift of the mouse monoclonal affinity column, R. Clark for the affinity purification protocol, M. Wu and Associates for oocyte injections, A. Sampson-Johannes for human peripheral blood lymphocytes, D. Lowy for useful discussions, and W. Bloch for critical review of the manuscript.

18 June 1987; accepted 10 August 1987

Germline Organization of the Murine T Cell Receptor β-Chain Genes

HUBERT S. CHOU, CHRISTOPHER A. NELSON, SANDIP A. GODAMBE, DAVID D. CHAPLIN, DENNIS Y. LOH

The complete germline organization of the β-chain genes of the murine T cell receptor was elucidated in order to obtain the structural basis for understanding the mechanisms of somatic DNA rearrangements. Twenty of the 22 known variable (V_β) genes are clustered within 250 kilobases of DNA 5′ to the constant region (C_β) genes. These V_β genes share the same transcriptional orientation as the diversity (D_β), joining (J_β), and C_β genes, which implies that chromosomal deletion is the mechanism for most V_β to D_β-J_β rearrangements. Within this V_β cluster, the distance between the most proximal V_β gene and the D_β-J_β-C_β cluster is 320 kilobases, as determined by field-inversion gel electrophoresis. The large distance between V_β and D_β, relative to that between D_β and J_β, may have significant implications for the ordered rearrangement of the T cell receptor β-chain genes.

THE VERTEBRATE IMMUNE SYSTEM uses multiple rearranging gene families to generate clonal diversity for its antigen-specific receptors. These gene families, including the heavy- and light-chain (κ and λ) genes of the B cell receptor (immunoglobulin) and the α-, β-, and γ-chain genes of the T cell receptor, undergo developmentally regulated somatic DNA rearrangements to generate functional transcription units during B cell or T cell differentiation (*1*). T cell receptors involved in the recognition of antigen and major histocompatibility complex molecules are disulfide-linked heterodimers composed of α and β chains, each divided into variable (V) and constant (C) regions (*2*). The V region of the β chain, like that of the immunoglobulin heavy chain, is encoded by three separate DNA segments, V_β, diversity (D_β), and joining (J_β), that recombine somatically to form a complete V_β gene (*3, 4*). The β-gene family contains two closely linked C_β genes,

Howard Hughes Medical Institute, Division of Immunology and Genetics, Department of Medicine, and Department of Microbiology and Immunology, Washington University School of Medicine, St. Louis, MO 63110.

$C_\beta 1$ and $C_\beta 2$, each of which is preceded by a cluster of six functional J_β gene segments and a single D_β gene segment (*5*).

Analyses of the murine T cell receptor β-chain genes to date have identified 22 V_β genes, belonging to 17 non–cross-hybridizing subfamilies (*6–8*). Of these V_β genes, $V_\beta 14$ has been mapped 10 kb 3′ to the $C_\beta 2$ gene, has an inverted transcriptional orientation relative to the D_β-J_β-C_β gene cluster, and undergoes somatic DNA rearrangement by chromosomal inversion (*9*). In contrast, the majority of the V_β genes are thought to lie 5′ to the C_β genes and to undergo rearrangement by the deletion of intervening chromosomal DNA. We have described a chromosomal order of 12 V_β genes by using deletion mapping in a T cell clone that had rearranged the β-gene locus on both chromosomes (*10*). To further investigate the mechanisms by which clonal diversity of the T cell receptor is generated, we have analyzed the overall structure of the β-gene locus by isolating overlapping cosmid clones and by mapping with field-inversion gel electrophoresis.

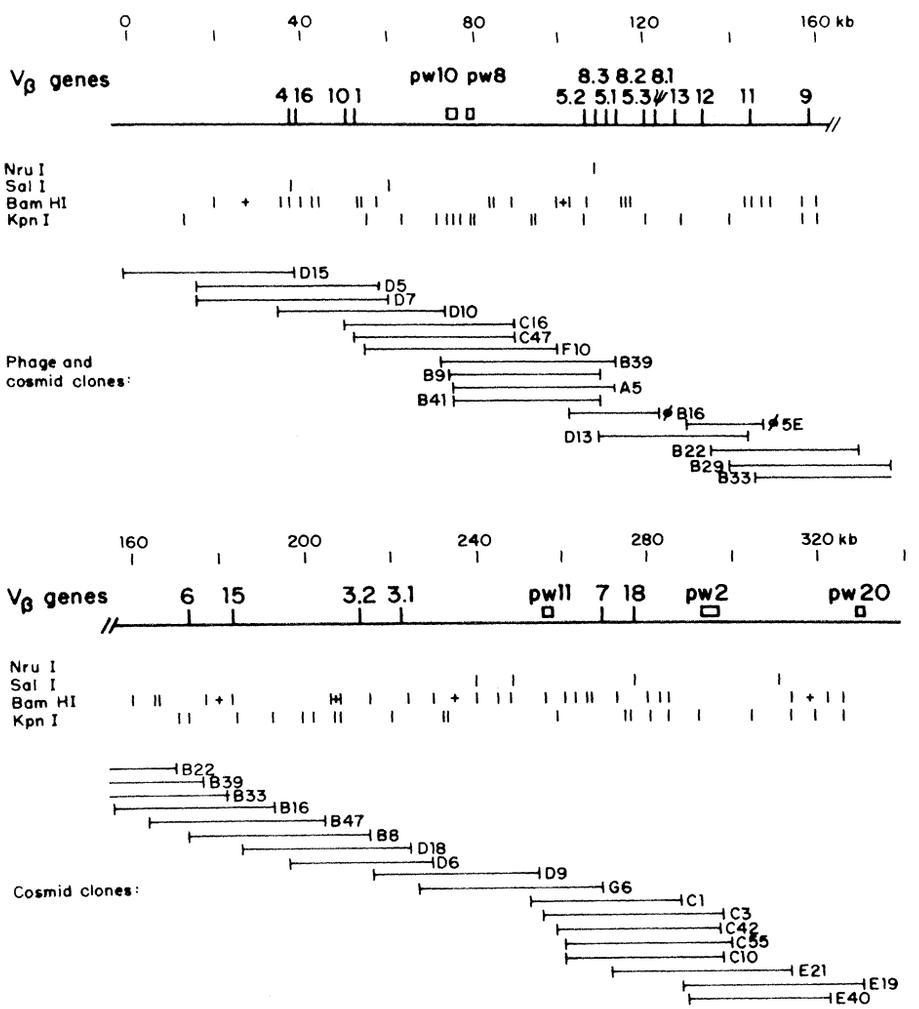

Fig. 1. Molecular map of 330 kb of the V_β gene locus of the murine T cell receptor. The V_β genes are shown as vertical lines above the horizontal line. V_β nomenclature is as described (*7, 13*). $V_\beta 3.1$ is the $V_\beta 3$ gene previously reported [also designated $V_\beta 2B4$ (*4*) and $V_\beta 3H.25$ (*24*)]; $V_\beta 3.2$ represents an additional V_β gene cross-hybridizing with the $V_\beta 3$ probe and is the BALB/c allele of the $V_\beta 17b$ reported by Kappler *et al.* (*25*). $V_\beta 18$ hybridizes to a V-region probe from a complementary DNA clone pM1pr2 (*8*); sequence determination indicates that $V_\beta 18$ is a functional V_β gene. The 5′ to 3′ transcriptional orientation is from left to right and is the same for all V_β genes shown. The single-copy probes used in the chromosomal walks are represented by open boxes above the horizontal line. These probes are as follows: pw10, a 1.8-kb Kpn I fragment from the 5′ end of clone B39; pw8, a 1.3-kb Eco RI fragment from the 3′ end of clone C16; pw11, a 1.7-kb Hind III fragment from the 5′ end of clone C1; and pw2, a 750-bp Eco RI–Hind III fragment from the 3′ end of clone C55. An additional single-copy probe, pw20, a 600-bp Ava II fragment from the 3′ end of clone E19, was used as a probe in determining the distance between the V_β and C_β genes. Phage clone 5E was a $V_\beta 11$-positive clone isolated from a total genomic library constructed from C57BL/6 liver DNA (*26*). Phage clone B16 has been described (*10*). Cosmid libraries were constructed from high molecular weight BALB/c liver DNA in the pTCF vector and were screened according to the method of Chaplin *et al.* (*11*).

The murine V_β genes were isolated by means of 16 V_β-specific probes to screen cosmid genomic libraries constructed from BALB/c liver DNA (*11, 12*). Twenty-four overlapping cosmid clones, which define three regions of approximately 60, 110, and 70 kb of DNA, were isolated. Twelve additional clones were obtained from two successive chromosomal walks performed with single-copy probes pw2, pw8, pw10, and pw11 isolated from the 3′ end of cosmid clone C55, the 3′ end of C16, the 5′ end of B39, and the 5′ end of C1, respectively. Together, these 36 overlapping cosmid clones span 330 kb of genomic DNA and contain 20 V_β genes previously described (Fig. 1). Two overlapping cosmid clones containing the $V_\beta 2$ gene and 12 overlapping clones containing the D_β, J_β, C_β genes were also isolated.

The distance between neighboring V_β genes ranges from 0.5 kb between $V_\beta 4$ and $V_\beta 16$ to 50 kb between $V_\beta 1$ and $V_\beta 5.2$. Thus, although there are regions with clustered V_β genes, there are also regions devoid of identified V_β genes. Whether the latter contain V_β genes not yet identified awaits further studies. The transcriptional polarity of these V_β genes was determined by restriction enzyme mapping and by direct DNA-sequence analysis. The 5′ to 3′ transcriptional polarity of each of the V_β genes within the 330-kb genomic segment is identical.

Mutant mice, including the SJL, C57L, C57BR, and SWR strains, which have an SJL type of T cell receptor, have been shown to lack 50% of the V_β genes and to have lost the reactivity with a V_β-specific serological reagent, KJ16-133 (*13, 14*). The fact that all ten V_β genes deleted in the SJL mouse are present in one contiguous region of DNA suggests that a single chromosomal deletion event led to the generation of the SJL-type V_β mutants. The breakage points of the SJL deletion occurred between $V_\beta 1$ and $V_\beta 5.2$ on the 5′ end and between $V_\beta 9$ and $V_\beta 6$ on the 3′ end (Fig. 2C). Thus, the SJL V_β mutant represents a deletion of 60 to 120 kb of DNA. The molecular basis of this deletion is not yet known.

Next, we determined the distance between the V_β and the D_β, J_β, and C_β genes and their relative transcriptional polarity. Chromosomal walking with cosmid clones extended the cloned genomic DNA 60 kb beyond the 3′ end of $V_\beta 7$ and 30 kb beyond the 5′ end of the $D_\beta 1.1$ gene. These two ends, however, did not overlap. Further analysis was performed with the field-inversion gel electrophoresis technique (*15, 16*).

Linkage between the V_β genes and the D_β, J_β, and C_β genes was obtained by mapping with two restriction enzymes.

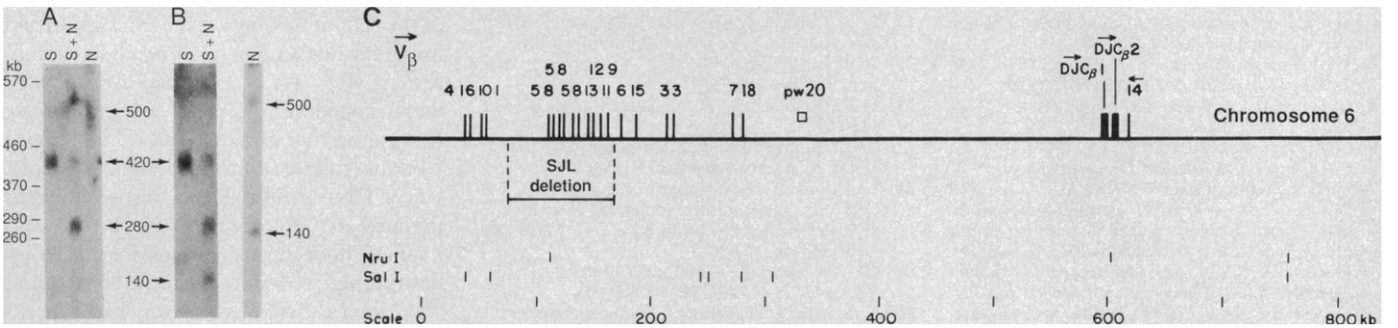

Fig. 2. Field-inversion gel-electrophoresis analysis of the β-chain locus of the T cell receptor. (**A**) Electrophoresed DNA samples were hybridized with a single-copy probe pw20, isolated from the 3′ end of clone E19 (see Fig. 1). The restriction enzymes used were Nru I (N) and Sal I (S). The size markers (yeast chromosomes, strain AB972) are indicated on the left. Hybridizing bands are marked on the right by arrows. (**B**) Gel containing electrophoresed DNA samples from (A) was treated with 0.1*N* NaOH to remove bound radioactive probe and rehybridized with a C_β-specific probe (lane S and lane S + N). The 420-kb fragment in lane S + N was a product of Nru I partial digestion. No fragments smaller than 140 kb were ever observed. (The 420-kb fragment in lane S and the 140-kb fragment in lanes S + N and N also hybridized to a $V_\beta 14$ probe.) (**C**) Schematic representation of the β-chain gene locus of the murine T cell receptor. V_β and C_β genes are shown as vertical lines or boxes above the horizontal lines. Restriction enzymes sites were derived from mapping of cosmid clones and from Southern blot analysis and are indicated by vertical lines below the horizontal line.

High molecular weight genomic DNA samples were digested with restriction enzymes, separated by field-inversion gel electrophoresis, and hybridized directly in the gel with single-copy probes from the V_β and C_β regions (*10, 17*). Southern blots of Nru I–restricted genomic DNA showed that two Nru I fragments, a 500-kb fragment and a 140-kb fragment, hybridized to a C_β probe (Fig. 2). The 500-kb Nru I fragment also hybridized to a $V_\beta 7$ probe. Mapping of rare restriction enzyme sites on cosmid DNA revealed one Nru I site in the $V_\beta 8.3$ gene and another Nru I site between the $C_\beta 1$ and $C_\beta 2$ genes. Thus, 500 kb is likely the distance between these two Nru I sites. Southern blots of Sal I–restricted genomic DNA indicated that a 420-kb Sal I fragment hybridized to both a C_β probe and a single-copy probe, pw20, isolated from the 3′ end of the 330-kb V_β gene cluster. In addition, Southern blots of double-digested (Nru I and Sal I) genomic DNA showed that a single 280-kb Nru I–Sal I fragment hybridized to both the pw20 and the C_β probes (Fig. 2, A and B). Mapping on cosmid DNA revealed that the 3′-most Sal I site in the 330-kb V_β cluster is located 30 kb 3′ to $V_\beta 18$ and 200 kb from the Nru I site in $V_\beta 8.3$. Therefore, the distance between the $V_\beta 18$ and $D_\beta 1.1$—that is, the smallest V_β to D_β-J_β rearranging distance—is 320 kb (Fig. 2C).

The observations that $V_\beta 7$ and $V_\beta 18$ are mapped closer to the C_β genes than is $V_\beta 4$ and that $V_\beta 7$ and $V_\beta 18$ are mapped closer to $C_\beta 1$ than to $C_\beta 2$ demonstrate that most V_β genes are located on the 5′ side of the D_β, J_β, and C_β genes and share the same transcriptional orientation. From these data and the data of the V_β deletion studies, we conclude that chromosomal deletion is the mechanism for most of the V_β to D_β-J_β rearrangements.

The order of V_β genes on the chromosome was initially hypothesized by V_β deletion mapping (*10*). The physical linkage map presented here establishes unequivocally the chromosomal order of the V_β, D_β, J_β, and C_β genes. The location of the $V_\beta 2$ gene (E1) has not been mapped (*6*). However, the fact that $V_\beta 2$ is present in the T cell clone F3 suggests that $V_\beta 2$ is located either 5′ to most V_β genes or 3′ to the $C_\beta 2$ and $V_\beta 14$ genes. Preferential rearrangement and utilization of immunoglobulin V_H genes in early B cell ontogeny have been correlated with their chromosomal position (*18*). Examination of RNA transcript levels in adult mice by ribonuclease protection assay did not reveal obvious preferential V_β usage (*19*). It would be interesting to determine whether V_β expression in the developing fetal thymus correlates with chromosomal position.

The tissue- and stage-specific expression of appropriate antigen receptors on immunocompetent B and T cells requires developmental regulation of the somatic recombination events. In the assembly of both the heavy-chain genes and the β-chain genes, an intermediate DJ rearrangement (D_HJ_H or $D_\beta J_\beta$) occurs before V_H to D_HJ_H or V_β to $D_\beta J_\beta$ rearrangement (*20, 21*). We note that the V_β to $D_\beta J_\beta$ rearranging distance (300 to 600 kb) is significantly larger than the D_β to J_β rearranging distance (1 to 10 kb). Thus, a larger rearranging distance is correlated with a later rearrangement event. Recent recombinase substrate studies have led to the hypothesis that the regulation of the accessibility of the target gene locus to a common recombinase determines the tissue and stage specificity of immunoglobulin and T cell receptor V-gene assembly (*22*). We suggest that the large distance between V and D genes might be necessary to ensure that the V-gene locus remains inaccessible to recombinase activity prior to DJ rearrangement. The presence of inappropriate DJ rearrangements (*23*) ($D_\beta J_\beta$ in precursor B cells and D_HJ_H in developing T cells) and the absence of inappropriate V to DJ rearrangements suggest that modulating the accessibility of the appropriate V-gene locus, and hence its rearrangement, is an important regulatory step. The existence of a large V to DJ distance also raises the intriguing possibility that this interval may encode other regulatory elements that contribute to the ultimate control of the tissue and stage specificity of V-region gene assembly.

REFERENCES AND NOTES

1. M. Kronenberg, G. Siu, L. Hood, N. Shastri, *Annu. Rev. Immunol.* **4**, 529 (1986); S. Tonegawa, *Nature (London)* **302**, 575 (1983); G. D. Yancopoulos and F. W. Alt, *Annu. Rev. Immunol.* **4**, 339 (1986).
2. J. P. Allison, B. W. McIntyre, D. Bloch, *J. Immunol.* **129**, 2293 (1982); K. Haskins *et al.*, *J. Exp. Med.* **157**, 1149 (1983); S. C. Meuer *et al.*, *ibid.*, p. 705.
3. G. Siu *et al.*, *Cell* **37**, 393 (1984).
4. Y.-h. Chien, N. R. J. Gascoigne, J. Kavaler, N. E. Lee, M. M. Davis, *Nature (London)* **309**, 322 (1984).
5. M. Malissen *et al.*, *Cell* **37**, 1101 (1984); N. R. J. Gascoigne, Y.-h. Chien, D. M. Becker, J. Kavaler, M. M. Davis, *Nature (London)* **310**, 387 (1984); G. Siu *et al.*, *ibid.* **311**, 387 (1984); J. Kavaler, M. M. Davis, Y.-h. Chien, *ibid.* **310**, 421 (1984).
6. P. Patten *et al.*, *Nature (London)* **312**, 40 (1984).
7. R. K. Barth *et al.*, *ibid.* **316**, 517 (1985); M. A. Behlke *et al.*, *Science* **229**, 566 (1985).
8. P. A. Singer, R. J. McEvilly, D. J. Noonan, F. J. Dixon, A. N. Theofilopoulos, *Proc. Natl. Acad. Sci. U.S.A.* **83**, 7018 (1986).
9. M. Malissen *et al.*, *Nature (London)* **319**, 28 (1986); In the murine γ-chain gene system, the V_γ and $C_\gamma 4$ gene segments are linked within 11 kb of each other [A. Iwamoto *et al.*, *J. Exp. Med.* **163**, 1203 (1986)].
10. H. S. Chou *et al.*, *Proc. Natl. Acad. Sci. U.S.A.* **84**, 1992 (1987).
11. D. D. Chaplin *et al.*, *ibid.* **80**, 6947 (1983).
12. Briefly, gel eluted V_β probes were radiolabeled to a specific activity of 1×10^9 to 2×10^9 cpm/μg by the random priming method of A. Feinberg and B. Vogelstein [*Anal. Biochem.* **132**, 6 (1983)]. Duplicate filters were initially hybridized with a mixture of four V_β probes and subsequently hybridized with additional probes after hybridizing colonies were picked from master filters. Cosmid filter hybridiza-

tion, colony purification, and cosmid DNA isolation were performed as described (*11*).
13. M. A. Behlke, H. S. Chou, K. Huppi, D. Y. Loh, *Proc. Natl. Acad. Sci. U.S.A.* **83**, 767 (1986).
14. G. Sim and A. Augustin, *Cell* **42**, 89 (1985); M. A. Behlke *et al.*, *J. Exp. Med.* **165**, 257 (1987).
15. G. F. Carle *et al.*, *Science* **232**, 65 (1986).
16. C. L. Smith *et al.*, *Methods Enzymol.*, in press.
17. High molecular weight DNA from BALB/c 3T3 fibroblasts was prepared in agarose blocks and digested with restriction enzymes according to the protocols of Carle *et al.* (*15*) and of Smith *et al.* (*16*). Restricted DNA samples were separated in a standard horizontal gel electrophoresis apparatus at 7 V/cm with the use of a programmable power inverter (Green Mountain Lab Supply). The power inverter was programmed as follows: initial forward time 1.0 second, forward increment 0.4 second, initial reverse time 0.5 second, and reverse increment 0.1 second, with a return to the initial settings after every 100 cycles of forward-reverse. Electrophoresis was performed for 14 to 16 hours at 15°C. Yeast chromosomes and a λ phage ladder were included as size markers. Separated DNA fragments were then hybridized directly in the gel as described previously (*10*).
18. G. D. Yancopoulos *et al.*, *Nature (London)* **311**, 727 (1984); G. E. Wu and C. J. Paige, *EMBO J.* **5**, 3475 (1986); R. M. Perlmutter, J. F. Kearney, S. P. Chang, L. E. Hood, *Science* **227**, 1597 (1985).
19. R. D. Garman, J. Ko, C. D. Vulpe, D. H. Raulet, *Proc. Natl. Acad. Sci. U.S.A.* **83**, 3987 (1986).
20. W. Born, J. Yagüe, E. Palmer, J. Kappler, P. Marrack, *ibid.* **82**, 2925 (1985).
21. M. G. Reth and F. W. Alt, *Nature (London)* **312**, 418 (1984).
22. G. D. Yancopoulos, T. K. Blackwell, H. Shuh, L. Hood, F. W. Alt, *Cell* **44**, 251 (1986).
23. Y. Kurosawa *et al.*, *Nature (London)* **290**, 565 (1981); A. Alessandrini, J. H. Pierce, D. Baltimore, S. V. Desiderio, *Proc. Natl. Acad. Sci. U.S.A.* **84**, 1799 (1987).
24. J. Goverman *et al.*, *Cell* **40**, 859 (1985).
25. J. Kappler, *et al.*, *ibid.* **49**, 263 (1987).
26. H. S. Chou *et al.*, *EMBO J.* **5**, 2149 (1986).
27. After submission of this manuscript, reports consistent with the direct deletional model have appeared: S. Fujimoto and H. Yamagishi, *Nature (London)* **327**, 242 (1987); K. Okazaki, D. D. Davis, H. Sakano, *Cell* **49**, 477 (1987).
28. We thank G. Carle, M. Olson, and M. R. Pozzi for advice on field-inversion gel electrophoresis, S. Anderson and M. Louie for critical comments on the manuscript, and D. London for manuscript preparation. This work was supported by funds from Howard Hughes Medical Institute (to D.D.C. and D.Y.L.) and Medical Scientist Training Grant GM07067 (to Washington University; H.S.C.).

18 May 1987; accepted 9 July 1987

Nuclear Reassembly Excludes Large Macromolecules

JOEL A. SWANSON AND PAUL L. MCNEIL

Interphase nucleus and cytoplasm are distinct compartments, whose soluble macromolecular contents mix when the nuclear envelope disassembles at mitosis. To determine how their interphase identities are reestablished, fibroblasts were loaded with fluorescent dextrans and then allowed to divide. Large dextrans (molecular weight of 40,000 or more) were excluded from condensed mitotic chromosomes and from newly formed, postmitotic interphase nuclei. Therefore, postmitotic reassembly of the nucleus as a compartment distinct from cytoplasm occurs by exclusion not only of organelles but also of soluble macromolecules. This might occur by exclusion of macromolecules from condensed chromatin throughout mitosis and completion of nuclear envelope assembly before nuclear expansion.

DURING MITOSIS THE NUCLEAR ENvelope of metazoan cells disassembles, and nucleoplasm mixes with cytoplasm. Yet interphase nucleoplasm and cytoplasm are distinct compartments, whose separate identities are maintained in part by the integrity of the nuclear envelope. Pores in the nuclear envelope provide a size-selective barrier to diffusion, confining many macromolecules (*1*) and organelles to the cytoplasm. Some large proteins are selectively concentrated in the nucleus (*2*), probably by specific transport or trapping mechanisms. Others, such as tubulin, are predominantly cytoplasmic (*3*). It is not known how, after mitosis, the distinct chemical identities of interphase nucleus and cytoplasm are reestablished. We examined this question by characterizing qualitatively and quantitatively the nucleocytoplasmic distribution of large fluorescent dextrans, initially confined predominantly to the cytoplasm, in cells that have undergone mitosis.

Dextrans labeled with fluorescein isothiocyanate (FDx) are highly water soluble molecules of low charge density that appear not to interact significantly with intracellular components or to affect cell viability (*4*). Moreover, they are available in various size ranges and are therefore useful as probes of the nucleocytoplasmic distribution of soluble macromolecules (*5*).

Dextrans were loaded into fibroblast (Swiss 3T3) cytoplasm by a modification of the scrape-loading technique (*6*). We denuded zones of cells from a monolayer by scratching the culture substratum with a sharp instrument (*7*). When the monolayer was wounded by scratching in the presence of large macromolecules such as FDx or Texas Red–labeled dextran (TRDx), many of the cells remaining on the substratum and lining the denuded zone were rendered fluorescent (Fig. 1); that is, they were loaded with exogenous molecules present during the culture wounding. Cells lining such wounds migrate into the denuded zone where DNA synthesis and mitosis are then initiated (*8*). We observed that loaded cells retained fluorescent dextrans for up to 48 hours, migrated into the denuded region, and divided, confirming for loaded cells these earlier observations of viability of cells bordering a wound. Therefore, by means of this "scratch-loading" procedure we were able to introduce the dextran probes into cell cytoplasm and, at the same time and in the same cells, to induce cell division. Scratch-loading, like microinjection and scrape-loading, relies on transient disruption of the plasma membrane. In all these methods, resealing of plasma membrane is evidenced by prolonged retention or exclusion of soluble dyes. More rigorous, long-term indications of cell health are movement and division. Scratch-loaded cells, like scrape-loaded (*6*) and microinjected cells, fulfill all these criteria. Moreover, the nuclear envelope permeability in undivided cells loaded by scratching was similar to that reported for microinjected cells (*5*). Scratch-loading should find many applications in cell biology, as it is a simple and rapid alternative to microinjection that requires only a small volume of dissolved macromolecules to be loaded.

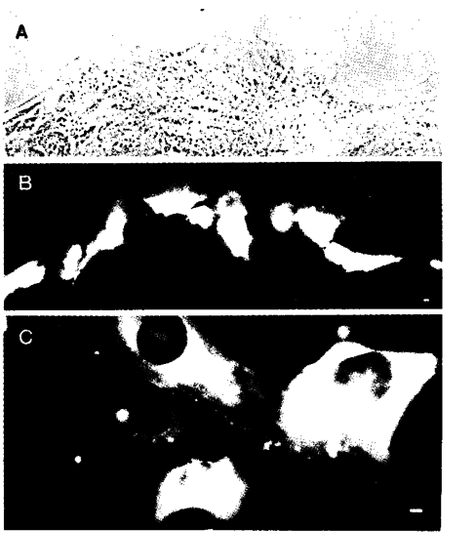

Fig. 1. Swiss 3T3 fibroblasts, 60 minutes after scratch-loading with fluorescent dextrans. (**A**) Phase-contrast images of cells bordering a denuded zone. (**B**) Fluorescein fluorescence image of cells in (A) that were scratch-loaded in the presence of FDx10, showing inclusion in the nucleus of this 10,000 molecular weight dextran. (**C**) Fluorescein fluorescence of cells scratch-loaded in the presence of FDx150, with exclusion from the nucleus of this 150,000 molecular weight dextran. Scale bars, 5 μm.

Department of Anatomy and Cellular Biology, Harvard Medical School, Boston, MA 02115.